

Low-temperature structural phase transition in a Cd_6Y 1/1 approximant

R. Tamura,¹ K. Edagawa,² C. Aoki,¹ S. Takeuchi,¹ and K. Suzuki²

¹Department of Materials Science and Technology, Tokyo University of Science, Noda, Chiba 278-8510, Japan

²Institute of Industrial Science, The University of Tokyo, Komaba, Meguro-ku, Tokyo 153-8505, Japan

(Received 29 May 2003; revised manuscript received 17 September 2003; published 13 November 2003)

Electron and x-ray-diffraction studies have revealed that a Cd_6Y 1/1 crystalline approximant ($Im\bar{3}$, $a = 1.5482$ nm) undergoes a phase transition at some temperature around 160 K. The transition accompanies a change of the lattice period as well as an extremely small tetragonal distortion ($c/a = 0.9992 \pm 0.0002$). Differential scanning calorimetry experiment also exhibits an anomaly around 175 K and the transition entropy suggests that the transition is of the order-disorder type with respect to the orientation of the Cd tetrahedron situated inside the icosahedral cluster. The phenomenon is discussed within the formalism of the Landau theory and it is suggested that the transition is attributed to an irreducible representation at the zone-boundary (N point) and the low-temperature phase possesses an orthorhombic $2a \times 2a \times a$ superlattice.

DOI: 10.1103/PhysRevB.68.174105

PACS number(s): 64.60.Cn, 61.44.Br, 61.14.-x, 61.10.Nz

I. INTRODUCTION

Cd_6Y^1 is a (1/1,1/1,1/1) rational approximant to the recently discovered $\text{Cd}_{5.7}\text{Yb}^2$ and $\text{Cd}_{17}\text{Ca}_3^3$ icosahedral phases. It has been reported¹ that Cd_6Y has a bcc structure with $a = 1.5482$ nm and belongs to the same space group ($Im\bar{3}$) as Cd_6Yb^4 and Cd_6Ca^5 approximants. The structure can be described as a bcc packing of an icosahedral cluster, which consists of four successive shells as depicted in Fig. 1. One of the interesting features common to the Cd_6Y -type compounds is the orientational disorder of the Cd tetrahedron located at the center of the icosahedral cluster at room temperature. In the case of Cd_6Y , six orientations of the Cd tetrahedron randomly occur at the vertex and the body center of the unit cell, while two orientations are statistically distributed in the case of Cd_6Yb , both resulting in the space group $Im\bar{3}$. In the case of Cd_6Yb and Cd_6Ca , it has been found^{6,7} that both the electrical resistivity and the specific heat exhibit a distinct anomaly at 110 K and 100 K, respectively, indicating an occurrence of a phase transition. In these compounds, the estimated transition entropies are close to $k_B \ln 4$ per unit cell, suggesting that the transition is of the order-disorder type with respect to the orientation of the Cd tetrahedra. By contrast, no distinct anomaly has been observed in the resistivity of Cd_6Y . However, detailed studies by electron and x-ray-diffraction experiments at low temperatures have shown an occurrence of a phase transition at some temperature around 160 K in Cd_6Y .

In this paper, we report the experimental evidence of the structural phase transition of Cd_6Y by means of electron, x-ray-diffraction, and differential scanning calorimetry (DSC) measurements. The phase-transition phenomenon will be discussed in terms of the Landau theory of continuous transitions and a comparison with other Cd_6Y -type compounds will also be made.

II. EXPERIMENT

Pure elements of Cd (6*N*) and Y (3*N*) near nominal composition Cd_6Y were melted at 973 K for 24 h in an alumina

crucible sealed inside a quartz tube under an argon atmosphere and then were slowly cooled from the melt at the rate of -1 K/h to obtain single grains. Single grains of centimeter size were successfully produced and they exhibit clearly defined facets as shown in Fig. 2(a). The characterization of the samples was performed by the backscattering x-ray Laue method. Figure 2(b) presents a Laue pattern taken from a $\{100\}$ surface, showing twofold rotational symmetry consistent with the space group $Im\bar{3}$. The obtained single grains were surrounded by $\{100\}$ and $\{110\}$ surfaces and the x-ray-diffraction measurements were performed for $\{100\}$ surfaces after removing the Cd matrix on the surfaces by mechanically polishing. The phase purity of the samples was confirmed by powder x-ray-diffraction measurements and scanning electron microscopy with energy-dispersive spectroscopy. The electrical resistivity was measured from 2 K to room temperature by a four-terminal ac bridge. The DSC measurement was carried out using Bruker DSC3200S in the temperature range from 110 to 300 K with a scanning rate of ± 10 K min^{-1} . X-ray-diffraction experiments with Cu $K\alpha$ have been performed using a Philips X³-Pert PRO x-ray diffractometer equipped with a cooling attachment (TTK450) at temperatures between 80 and 300 K and the $K\alpha_2$ peaks were subtracted numerically from the raw data. TEM observations were performed using JEM2010F equipped with a liquid- N_2 cooling stage operating at an acceleration voltage of 200 kV.

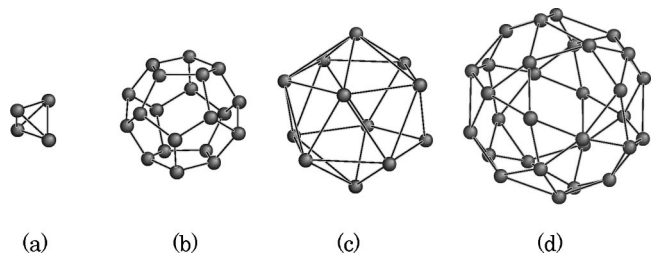


FIG. 1. The icosahedral cluster located at the vertex and the body center of the unit cell in the Cd_6Y crystal: (a) Cd_4 tetrahedron, (b) Cd_{20} dodecahedron, (c) Y_{12} icosahedron, and (d) Cd_{30} icosidodecahedron. The Cd_4 tetrahedron is orientationally disordered at room temperature.

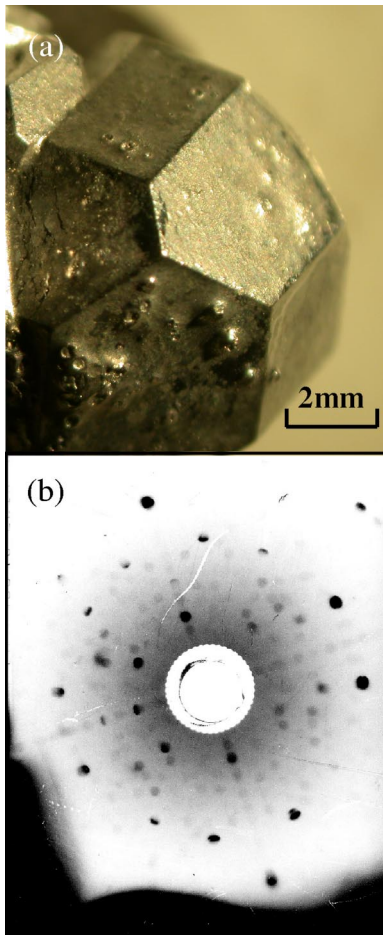


FIG. 2. (a) Photograph of a single-grain Cd_6Y grown from the melt. Clearly defined rectangular and hexagonal facets of the $\{100\}$ and $\{110\}$ surfaces, respectively, are seen. (b) Backscattering x-ray Laue photograph with an incidence perpendicular to the $\{100\}$ surface of a single-grain Cd_6Y .

III. RESULTS AND DISCUSSION

A. Electrical resistivity

Figure 3 presents the electrical resistivity of Cd_6Y as a function of temperature together with those of Cd_6Yb and Cd_6Ca for comparison. No sign of a phase transition is ob-

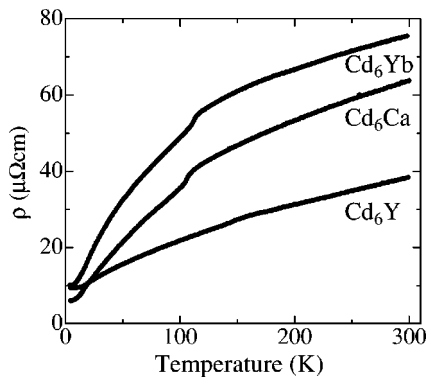


FIG. 3. Electrical resistivity of Cd_6Y as a function of temperature, together with those of Cd_6Yb and Cd_6Ca for comparison.

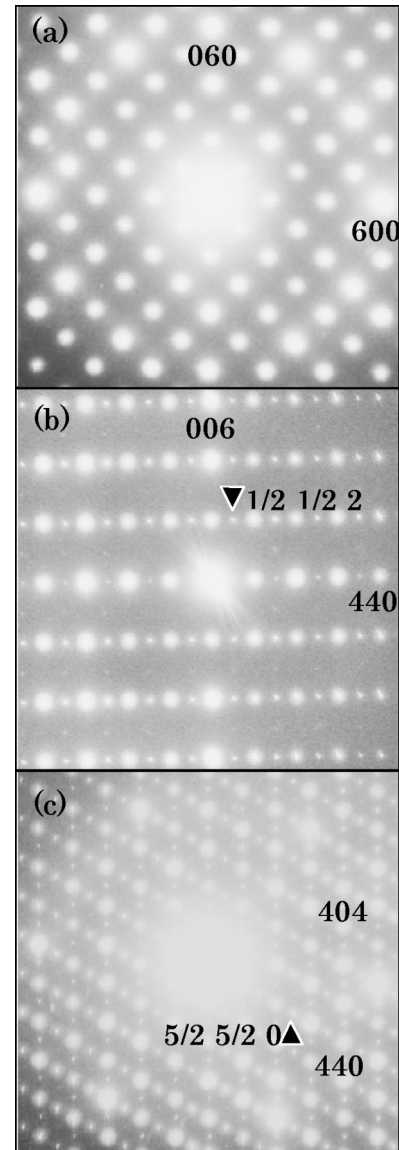


FIG. 4. Electron-diffraction patterns taken along (a) $[001]$, (b) $[1\bar{1}0]$, and (c) $[1\bar{1}\bar{1}]$ directions at 80 K.

served in the resistivity of Cd_6Y , whereas it clearly exhibits a sharp drop at 110 K and 100 K upon cooling for Cd_6Yb and Cd_6Ca , respectively. Such a drop of the resistivity in Cd_6Yb and Cd_6Ca has been attributed to ordering of the crystal structures, i.e., the orientational ordering of the Cd tetrahedron located at the vertex and the body center of the unit cell.^{6,7} By contrast, the resistivity is highly insensitive to the phase transition in the case of Cd_6Y , which had obscured the occurrence of the phase transition until the electron and x-ray-diffraction experiments were performed at low temperatures as presented in the subsequent sections.

B. Electron diffraction

Figure 4 presents the electron-diffraction patterns of Cd_6Y taken along $[001]$, $[1\bar{1}0]$, and $[1\bar{1}\bar{1}]$ directions at 80 K. We observe that superlattice reflections appear in a com-

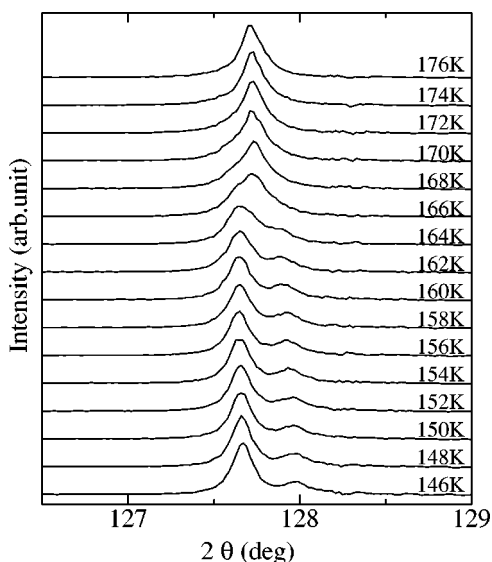


FIG. 5. X-ray-diffraction spectra around the (18 0 0) peak. The spectra were taken with decreasing temperature.

mensurate manner to the fundamental reflections, clearly indicating an occurrence of a phase transition at some temperature above 80 K. Here, no clear change of the fundamental spots is seen, which implies that the crystal structure is basically unchanged throughout the phase transition. The superlattice reflections are found to satisfy the condition $h, k = \text{half integers}$, which means that the lattice period is doubled below the transition temperature: Thus the low-temperature phase is either $2a \times 2a \times a$ or $2a \times 2a \times 2a$ superlattice. For the sake of the later discussion we note that it cannot be a face-centered (F-type) $2a \times 2a \times 2a$ superlattice since the observed reflections apparently do not satisfy the extinction rule of the F-type lattice. We also note that the disappearance of superlattice spots with h, k, l of all half integers in any of the incidences suggests that the $2a \times 2a \times a$ superlattice is more likely the case than the $2a \times 2a \times 2a$ superlattice. Another significant feature in Fig. 4 is that the three fold rotational symmetry is broken in the pattern of the $[1\bar{1}\bar{1}]$ incidence, indicating that the low-temperature phase is not cubic.

C. X-ray diffraction

Figure 5 presents x-ray-diffraction spectra around the (18 0 0) peak taken for a $\{100\}$ surface of Cd_6Y from 176 to 146 K, and Fig. 6 the lattice parameters as a function of temperature. We observe that upon cooling the (18 0 0) peak is split into two peaks at 164 K and, in addition, a slight discontinuity in the unit-cell volume of about 0.027% occurs at the transition. The splitting of the peak, i.e., breakdown of the cubic symmetry, is consistent with the breakdown of the threefold symmetry observed in Fig. 4(c). Here we note that the discontinuity in the unit-cell volume may not necessarily mean that the present transition is essentially of the first order, but it may occur as a consequence of a continuous transition. The point will be discussed later. From Fig. 5, it is seen that the lattice undergoes a small tetragonal distortion of

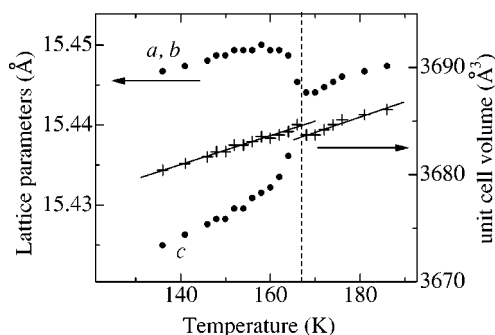


FIG. 6. Lattice parameters and the unit-cell volume of Cd_6Y as a function of temperature.

$c/a = 0.9992 \pm 0.0002$ at the transition. Such an extremely small lattice distortion manifests that the present phase transition is rather continuous and it seems reasonable to assume that the low-temperature phase belongs to a subgroup of the high-temperature phase ($Im\bar{3}$), which is either trigonal or orthorhombic. Among these two, the splitting of the (18 0 0) peak discards the former case and thus we are led to a conclusion that the low-temperature phase is orthorhombic. Furthermore, the splitting of the peak itself verifies that the crystal consists of domains below the transition temperature since a single crystal was used for the present study. The domain size is typically greater than 100 nm, which is about the radius of the incident electron beam used in the electron-diffraction experiments.

Figure 7 presents the integrated intensity of the (18 0 0) peak as a function of temperature. The peak intensity is found to increase upon cooling as 164 K, i.e., the onset temperature of the distortion, is approached, which is then followed by a substantial reduction as the tetragonal distortion sets in. The increase of the Bragg-peak intensity indicates that some kind of disorder diminishes during the transition above 164 K. Since the high-temperature phase possesses an averaged structure with respect to the orientation of the Cd tetrahedron, the orientational ordering of the tetrahedra may be responsible for such an increase of the Bragg-peak intensity. This point will be further discussed in the following section. On the other hand, the intensity decrease below 164 K is naturally understood as a result of lattice strain introduced by the tetragonal distortion.

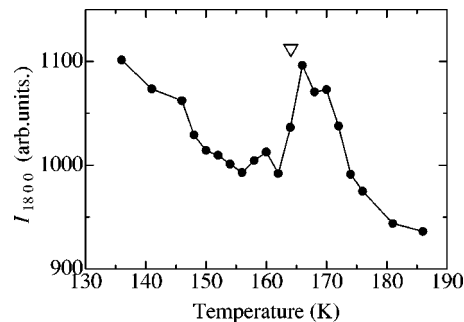


FIG. 7. The integrated intensity of the (18 0 0) peak of Fig. 5 as a function of temperature. The open triangle indicates the onset temperature of the lattice distortion.

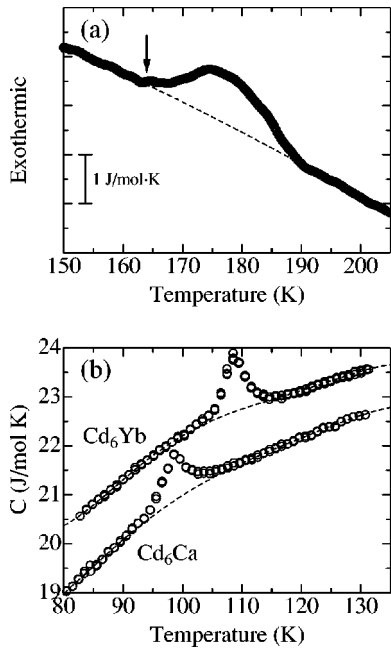


FIG. 8. (a) DSC trace of Cd_6Y with scanning rate of -10 K min^{-1} . (b) Specific heat of Cd_6Yb and Cd_6Ca . The arrow in (a) indicates the onset temperature of the tetragonal distortion. In (a) and (b), the broken lines indicate the assumed base lines which were subtracted from the experimental curves for the estimation of the transition entropies. Note that the scales in the both figures are set the same for the sake of better comparison.

D. Differential scanning calorimetry

Two types of mechanisms are known to exist for nearly continuous phase transitions; the order-disorder type and the displacive one. One way to distinguish them may be the estimation of the transition entropy ΔS , since it measures the degree of ordering associated with the phase transition. In the case of the order-disorder-type transition, the transition entropy is given by $\Delta S = k_B \ln \omega$, where ω is the number of possible configurations in the high-temperature phase. On the other hand, the transition entropy can be in principle zero in the case of the displacive-type transition. Figure 8(a) presents a DSC trace of Cd_6Y with a cooling rate of -10 K min^{-1} , and Fig. 8(b) the specific heats of both Cd_6Yb and Cd_6Ca for a comparison. As seen from Fig. 8(b), both Cd_6Yb and Cd_6Ca exhibit a distinctive peak at the temperatures corresponding to the resistivity anomalies and the transition entropies are estimated to be $1.03k_B$ and $1.15k_B$ per unit cell, i.e., $\omega = 1.7$ and 1.8 per tetrahedron, respectively. The fact that the values of ω are close to 2 suggests an occurrence of the order-disorder-type transition in these compounds. On the other hand, as seen from Fig. 8(a), a rather broad exothermic peak appears around 175 K in the case of Cd_6Y , which is at a somewhat higher temperature relative to the onset temperature of the tetragonal distortion. Accordingly, the transition entropy is obtained as $1.7k_B$ per unit cell, which corresponds to $\omega = 2.3$. Therefore it also suggests that the present phase transition is of the order-disorder type, i.e., two orientations of the tetrahedron which is located at the center of the icosahedral cluster become ordered in the low-

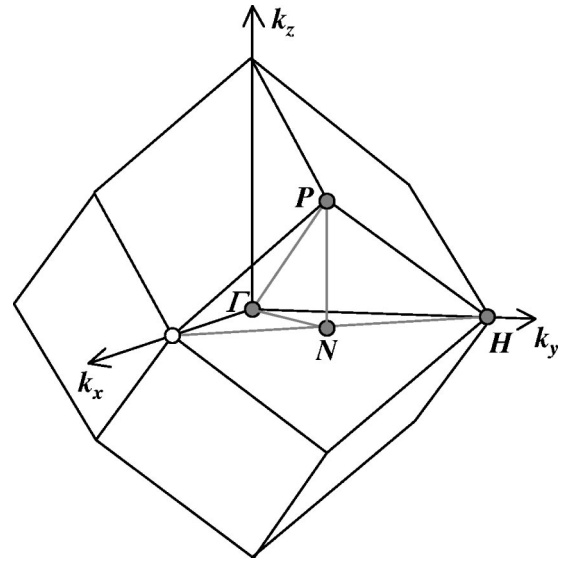


FIG. 9. Brillouin zone and the special points of $Im\bar{3}$.

temperature phase. We note that the increase of the Bragg-peak intensity on cooling above 164 K is well understood by this occurrence of the ordering in the crystal structure. In this view, the tetragonal distortion may be taken as a consequence of the ordering of the structure above 164 K, probably due to a symmetry change caused by the transition. According to the structural model of Cd_6Y^4 six orientations of the Cd tetrahedra are reported to exist, therefore one might expect that the transition entropy would be given by $\Delta S = k_B \ln 6$. The rather small transition entropy than expected might be attributed to two possible origins: One is that Cd_6Y might have the same cluster composition as Cd_6Yb and the other is that the Cd tetrahedra may not be completely ordered at the transition. With this respect, reexamination of the crystal structure of Cd_6Y is desirable to clarify this point.

E. Application of the Landau theory

Since the phase transition is rather continuous as evidenced by the extremely small tetragonal distortion ($c/a = 0.9992 \pm 0.0002$), it is plausible that the Landau theory⁸ of continuous transitions can describe the present transition. Within the formalism of the Landau theory, the active representations that can drive a continuous transition in $Im\bar{3}$ belong to the Γ , H , N , and P points of the Brillouin zone (see Fig. 9).⁹ Among them, the irreducible representations (irreps) which can bring about a change in the lattice periodicity are those of the N and P points, resulting in $2a \times 2a \times a$ or $2a \times 2a \times 2a$ superlattice. In the case of irreps at the P point, the resulting low-temperature phase would be F-type $2a \times 2a \times 2a$ superlattice. However, this is not the case for Cd_6Y since the low-temperature phase does not comply with the extinction rule of F-type lattice ($h, k, l =$ all even or odd) as mentioned above. On the other hand, both $2a \times 2a \times a$ and $2a \times 2a \times 2a$ superlattices are possible from irreps at the N point. Since the electron-diffraction experiments suggest that $2a \times 2a \times a$ superlattice is more likely, we are led to a conclusion that the phase transition is described by an irrep be-

longing to the N point and the low-temperature phase possesses an orthorhombic $2a \times 2a \times a$ superlattice.

IV. CONCLUSIONS

Electron- and x-ray-diffraction studies on a Cd_6Y approximant at low temperatures reveal that the $1/1$ approximant undergoes a structural phase transition at some temperature around 160 K. The phase transition accompanies an extremely small tetragonal distortion of the lattice together with a change of the lattice periodicity. Differential scanning calorimetry exhibits an anomaly around 175 K and the estimated transition entropy suggests that the present transition is of the order-disorder type, implying that the tetragonal distortion is a consequence of the ordering. By applying the Landau theory of continuous transitions, it is suggested that

the transition is attributed to an irreducible representation at the N point and low-temperature phase possesses an orthorhombic $2a \times 2a \times a$ superlattice.

ACKNOWLEDGMENTS

We would like to thank M. Miyake of Application Laboratory, PANalytical for her assistance in the x-ray-diffraction experiments, and S. Nagatani of Bruker AXS K.K. for her help in the DSC measurement. This work was supported in part by a Grant-in-Aid for Scientific Research (Grant No. 13750616) from the Japan Society for Promotion of Science and also by Core Research in Environmental Science and Technology (CREST), Japan Science and Technology Corporation.

¹A.C. Larson and D. Cromer, Acta Crystallogr., Sect. B: Struct. Crystallogr. Cryst. Chem. **B27**, 1875 (1971).

²A.P. Tsai, J.Q. Guo, E. Abe, H. Takakura, and T.J. Sato, Nature (London) **408**, 537 (2000).

³J.Q. Guo, E. Abe, and A.P. Tsai, Phys. Rev. B **62**, R14 605 (2000).

⁴A. Palenzona, J. Less-Common Met. **25**, 367 (1971).

⁵G. Bruzzone, Gazz. Chim. Italy **102**, 234 (1972).

⁶R. Tamura, Y. Murao, S. Takeuchi, M. Ichihara, M. Isobe, and Y.

Ueda, Jpn. J. Appl. Phys., Part 2 **41**, L524 (2002).

⁷R. Tamura, K. Edagawa, Y. Murao, S. Takeuchi, and K. Suzuki (unpublished).

⁸L.D. Landau and E.M. Lifshitz, *Statistical Physics*, 3rd ed. (Pergamon, Oxford, 1980), Pt. 1, Chap. XIV.

⁹D.M. Hatch and H.T. Stokes, Phys. Status Solidi B **130**, 79 (1985).